Hindawi
Complexity
Volume 2024, Article ID 7126978, 22 pages
https://doi.org/10.1155/2024/7126978

WILEY | Hindawi

Research Article

Adaptive Optimal Terminal Sliding Mode Control for T-S Fuzzy-Based Nonlinear Systems

Farzad Soltanian,[1,2] **Amir Parviz Valadbeigi**,[1,3] **Jafar Tavoosi**,[4] **Rahmat Aazami**,[4] **Mokhtar Shasadeghi**,[2] **Mohammadamin Shirkhani**,[4] **and Amirreza Azizi**[5]

[1]*Department of Electrical and Computer Engineering, University of Alberta, Edmonton, AB T6G 2M9, Canada*
[2]*Electrical Engineering Faculty, Shiraz University of Technology, Shiraz 715555-313, Iran*
[3]*Department of Electrical Engineering, Islamic Azad University, Khorramabad Branch, Khorramabad, Iran*
[4]*Department of Electrical Engineering, Ilam University, Ilam, Iran*
[5]*Department of Electrical Engineering, Shahed University of Tehran, Tehran, Iran*

Correspondence should be addressed to Farzad Soltanian; fsoltani@ualberta.ca and Jafar Tavoosi; j.tavoosi@ilam.ac.ir

Received 13 December 2023; Revised 10 March 2024; Accepted 8 April 2024; Published 25 April 2024

Academic Editor: Xiaoping Liu

This study utilizes the Takagi–Sugeno fuzzy model to represent a subset of nonlinear systems and presents an innovative adaptive approach for optimal dynamic terminal sliding mode control (TSMC). The systems under consideration encompass bounded uncertainties in parameters and actuators, as well as susceptibility to external disturbances. Performance evaluation entails the design of an adaptive terminal sliding surface through a two-step process. Initially, a state feedback gain and controller are developed using Linear Matrix Inequality (LMI) techniques, grounded on H_2-performance and partial eigenstructure assignment. Dynamic sliding gain is subsequently attained via convex optimization, leveraging the derived state feedback gain and the designed terminal sliding mode (TSM) controller. This approach diverges from conventional methods by incorporating control effort and estimating actuator uncertainty bounds, while also addressing sliding surface and TSM controller design intricacies. The TSM controller is redefined into a strict feedback form, rendering it suitable for addressing output-tracking challenges in nonlinear systems. Comparative simulations validate the effectiveness of the proposed TSM controller, emphasizing its practical applicability.

1. Introduction

Sector nonlinearity and approximation are two approaches which widly used to describe the Takagi–Sugeno (T-S) fuzzy model of a nonlinear system. the sector nonlinearity approach present an exact model of the nonlinear system. Additionally, it transforms the nonlinear system into a collection of local linear models through fuzzy blending [1–3]. This T-S fuzzy model proves valuable for characterizing uncertain nonlinear systems. Furthermore, addressing added uncertainties, like those associated with actuators, recent work has proposed integrating T-S model representation with sliding mode control (SMC) designs [4–7].

Sliding mode control is a well-established approach in robust control theory, particularly for handling known but bounded-matched uncertainty [8–10]. To extend its applicability to scenarios with unknown upper bounds [11, 12], adaptive methods have been explored for estimating uncertainty boundaries [13–15]. An example is presented in [16], which introduces an adaptive SMC design for a nonlinear suspension system with unknown bound uncertainty. Additionally, the Terminal Sliding Mode Control (TSMC) technique is frequently used to rapidly converge system dynamics to the sliding surface. Proper design of TSMC parameters ensures infinite stability of the closed-loop system [17–19]. In [20], an adaptive TSMC is developed

for a variable load DC-DC buck converter, where nonlinear sliding surface coefficients are adjusted to account for load resistance changes. An adaptive law is integrated to manage load fluctuations and achieve dynamic sliding along the surface. TSMC offers advantages such as swift response, disturbance resistance, and ease of implementation. Consequently, the focus of our literature analysis revolves around TSMC design for linear systems or TSFM, the fuzzy blending of local linear subsystems.

Various controller design methods exist for linear systems, such as Linear Quadratic Regulator (LQR), Pole Placement, Eigenvalue Assignment, and eigenstructure assignment techniques [21–24]. A comparative study [25] demonstrated that eigenstructure assignment yields fast, non-overshooting responses, outperforming other methods by enabling eigenvalue and eigenvector assignment. Combining different state feedback and robust approaches can enhance robust controller performance and achieve desired transient behavior in the presence of uncertainty or disturbance [26–29]. In [26], a blend of pole placement objectives an H_∞ performance is proposed. Also, combines eigenstructures assignment and H_2-characterization is presented in [27] for state feedback gain calculation, which is used to achieve sliding surface and control inputs. The definition of sliding surface significantly influences control system performance. In [28], a constrained bilinear quadratic regulator which is known as an optimal quadratic control problem was designed by a performance index. In [29], a combination of the sliding mode control (SMC) and nonlinear control law is proposed and the proposed controller parameter were optimized utilizing the particle swarm optimization (PSO) method [29].

Conversely, addressing output tracking control in nonlinear systems has long been a challenge [30–32]. Output signal convergence to reference signal was achieved in [33–35] through output feedback control. However, robustness against external disturbances was not fully considered. State and input constraints were incorporated in [36] for static output feedback control of T-S fuzzy systems. New design criteria were established using Finsler's lemma and fuzzy Lyapunov functions to ensure stabilizing controller existence. Further relaxed LMI conditions were obtained using slack variables. Nonetheless, this study lacked robustness against uncertainties, external disruptions, or optimized performance. Addressing these concerns, Köhler et al. [37] introduced a method for designing static output feedback controllers for constrained T-S fuzzy systems. The fuzzy control framework integrated Lyapunov stability theory to consider state and input constraints. The fuzzy control design was reformulated as an optimization problem with LMI constraints. Despite producing positive results, this study did not fully address controller robustness against uncertainty and external disturbances.

In the realm of control theory, recent advancements have addressed critical challenges in various domains. Paper [38] introduces a hybrid Q-learning method for adaptive fuzzy H_∞ control in discrete-time nonlinear Markov jump systems, offering innovative solutions to address complexities in solving fuzzy game-coupled algebraic Riccati equations (FGCAREs) [38]. However, despite its merits, this approach may encounter limitations in computational complexity and generalizability beyond Takagi–Sugeno fuzzy models [38]. Meanwhile, paper [39] proposes nonfragile H_∞ synchronization for discrete-time T-S fuzzy Markov jump systems, leveraging a novel matrix transformation method and nonfragile controller design [39]. While promising, challenges such as computational complexity and conservatism in criteria underscore the need for further research to enhance practical applicability and robustness [39]. Furthermore, investigations in sliding mode control (SMC) for discrete-time T-S fuzzy networked singularly perturbed systems, as explored in paper [40], highlight the integration of observer-based techniques to manage communication burdens and improve networked control system (NCS) effectiveness [40]. Nevertheless, complexities in implementation and limited applicability to certain system dynamics remain notable concerns [40]. Future endeavors may delve into stochastic time-delayed NCSs to bolster system performance and stability, mitigating these potential limitations [40]. These collective efforts reflect the ongoing pursuit to advance control methodologies, addressing real-world complexities and pushing the boundaries of system robustness and efficiency.

A literature review highlights the limited discussion on adaptive estimation of uncertainty boundaries combined with optimal TSMC based on T-S fuzzy systems. Building on the discussed advantages, this paper investigates an adaptive approach to design optimal TSMC for T-S fuzzy-based nonlinear systems. The proposed method involves online adjustment of the nonlinear sliding surface gain and adaptive TSM control input. Fuzzy rule consequences allocate local subsystems to desired negative values based on partial eigenstructure assignment. The study assumes unknown actuator uncertainty bounds, deriving an adaptive formula to determine these bounds. The TSMC design is a two-step process: proposing a new TSM control input and adaptive formula to find uncertainty bounds, followed by calculating suboptimal gains for each rule consequence using H_2-performance index and partial eigenstructure assignment likewise [41]. Convex combination identifies state feedback control associated with H_2-performance criteria and generalized partial eigenstructure assignment. An optimization problem determines the online optimal nonlinear sliding matrix gain. Extending this approach, the study addresses output tracking for strict feedback form nonlinear systems using the T-S fuzzy model, demonstrating effectiveness of the presented method through comparative simulations.

This paper presents an innovative approach to tackle the complex challenge of achieving optimal output tracking control in strict feedback nonlinear systems with unknown actuator uncertainty bounds, modeled using the TSFM. It introduces the concept of extending eigenstructure assignment to nonlinear systems, enabling the optimization of transient response characteristics by defining sliding surfaces and control inputs aligned with desired eigenvalues corresponding to local subsystems within fuzzy rule consequences. Additionally, this paper proposes the novel idea of online TSMC design, where the level of control effort is considered during sliding surface and control input design. Suboptimal gains are computed for each fuzzy rule consequence based on system and actuator uncertainty, as well as external disturbance, and then combined to derive a customized control law tailored to the specific

nonlinear system. Throughout the control design process, H_2-optimization techniques are applied to enhance transient response characteristics.

This paper is structured as follows. Section 2 introduces nonlinear systems with matched uncertainty subjected to external disturbance. Section 3 outlines major design processes and formulation derivations. Section 4 presents a comparative case study to showcase the strategy's effectiveness, followed by the conclusion in Section 5.

Hint herm$(\Delta) = \Delta + \Delta^*$, where Δ is a square matrix and Δ^* represents the conjugate transpose of Δ; Δ^T denotes the transpose of Δ. In addition, $\|\Delta\|$ denotes the Euclidean norm Δ.

2. Problem Statement and Preliminaries

Consider the following class of nonlinear systems with matched uncertainty that are subjected to external disturbance:

$$\begin{aligned}\dot{x}_1(t) &= x_2(t),\\ \dot{x}_2(t) &= f_1(x,t) + f_2(x,t)(u(t) + g(x,t)) \\ &\quad + f_3(x,t)w(t),\\ z(t) &= g_1(x(t),t)x(t) + g_2(x,t)(u(t) + g(x,t)),\end{aligned} \tag{1}$$

where the state vector, the H_2-performance output vector, the control input vector, the external disturbance input with bounded energy, and the actuator matched uncertainty with unknown bounded value $\rho(x,u,t)$ are denoted by $x \in \mathbb{R}^n$, $z \in \mathbb{R}^q$, $u \in \mathbb{R}^m$, $w \in \mathbb{R}^q$, and $g(x,t) \in \mathbb{R}^m$, respectively. Additionally, the nonlinear functions $f_1(x(t),t)$, $f_2(x(t),t)$, $f_3(x(t),t)$, $g_1(x(t),t)$, and $g_2(x(t),t)$ have suitable dimensions and undetermined parameter values. The fuzzy system can be used to represent the nonlinear system mentioned in (1) as follows.

2.1. Plant Rule i. If $\mu_1(t)$ is $F_{1,i}$ and . . .and $\mu_g(t)$ is $F_{g,i}$, then

$$\begin{aligned}\dot{x}_1(t) &= x_2(t),\\ \dot{x}_2(t) &= A_{s,i}x(t) + B_{1s,i}(u(t) + g(x,t)) + B_{2s,i}w(t),\\ z(t) &= C_i x(t) + D_i u(t); \quad i = 1,\ldots,r,\end{aligned} \tag{2}$$

where $\mu_j(t)$ and $F_{j,i}$ $(j = 1,\ldots,g)$ are the premise variables and fuzzy sets, respectively; r is standing the number of the fuzzy rules; and matrices $B_{1s,i} \in \mathbb{R}^{n_2 \times m}$; $B_{2s,i} \in \mathbb{R}^{n_2 \times q}$; $A_{si} \in \mathbb{R}^{n_2 \times n}$; $C_i \in \mathbb{R}^{q \times n}$; and $D_i \in \mathbb{R}^{q \times m}$ have appropriate dimensions. Furthermore, $x = \begin{bmatrix} x_1 & x_2 \end{bmatrix}^T$, $x_1 \in \mathbb{R}^{n_1}$, $x_2 \in \mathbb{R}^{n_2}$, $n_1 + n_2 = n$, and $n_1 = n_2$.

The overall T-S fuzzy model of the nonlinear system given in (1) will be inferred using a singleton fuzzifier, product inference, and center-average defuzzifier as follows:

$$\begin{aligned}\dot{x}_1(t) &= x_2(t),\\ \dot{x}_2(t) &= \sum_{i=1}^{r} h_i(\mu)\left\{A_{s,i}x(t) + B_{1s,i}(u(t) + g(x,t)) + B_{2s,i}w(t)\right\},\\ z(t) &= \sum_{i=1}^{r} h_i(\mu)\{C_i x(t) + D_i(u(t) + g(x,t))\},\end{aligned} \tag{3}$$

where $h_i(\mu)$ denotes the relative weighting value (normalized membership function), in which $h_i(\mu) \geq 0$ and $\sum_{i=1}^{r} h_i(\mu) = 1$ and

$$h_i(\mu) = \frac{\prod_{j=1}^{g} F_{j,i}\left(\mu_j(t)\right)}{\sum_{i=1}^{r}\prod_{j=1}^{g} F_{j,i}\left(\mu_j(t)\right)}, \tag{4}$$

where $F_{j,i}(\mu_j(t))$ represents the grade of membership of $\mu_j(t)$ in $F_{j,i}$. Following that, the T-S fuzzy controller will be designed in the same way as (1). Parallel Distributed Compensator (PDC) [1] is used to design the fuzzy controller $u(t)$ as follows.

2.2. Controller Rule i. If $\mu_1(t)$ is $F_{1,i}$ and . . .and $\mu_g(t)$ is $F_{g,i}$, then

$$u(t) = K_i x(t); \quad i = 1,\ldots,r, \tag{5}$$

where K_i indicates the feedback gain. The overall PDC controller can then be represented as

$$u(t) = \sum_{i=1}^{r} h_i(\mu(t))K_i x(t), \tag{6}$$

where $h_i(\mu)$ denotes the normalized fuzzy membership functions presented in (4).

3. Main Results

In this section, we employ the conventional methodology for designing control inputs in the context of nonlinear systems characterized by matched uncertainties and external disturbances to establish a sliding mode control input. The process entails the utilization of both a reaching control input and an equivalent control input, constituting the input strategy for the reaching and sliding phases, respectively. The standard control input design procedure itself is composed of two primary constituents. In cases where nonlinear systems are subject to matched uncertainty in the absence of external disturbances, we propose the adoption of the reaching control input as the initial step. Subsequently, in the second phase, the development of an equivalent control input is carried out for nonlinear systems exposed to external disturbances, employing state feedback control while ensuring alignment with the performance benchmarks of robust control design. These benchmarks encompass H_2-performance and eigenstructure assignment. As a result, during the process of designing the state feedback control input, we are empowered to address the challenge of robust control design for the Takagi–Sugeno fuzzy model when confronted with the presence of external disturbances. This is achieved by conscientiously incorporating considerations related to H_2-performance characterization and partial eigenstructure assignment. This section is methodically divided into three subsections. The first and second subsections delineate the formulation of a Terminal Sliding Mode (TSM) controller tailored to the Takagi–Sugeno fuzzy model. This formulation is rooted in the primary and subsequent stages of the conventional sliding mode control design methodology, respectively. The third subsection

subsequently delves into the intricate matter of output tracking.

3.1. Terminal Sliding Mode Controller Design. In the initial stage of our proposed development approach, it is imperative to consider the system state (3) when there is no external disturbance. This step is pivotal to the subsequent methodology.

$$\dot{x}_1(t) = x_2(t), \tag{7}$$

$$\dot{x}_2(t) = \sum_{i=1}^{r} h_i(\mu)\left\{A_{s,i}x(t) + B_{1s,i}(u(t) + g(x,t))\right\}, \tag{8}$$

$$z(t) = \sum_{i=1}^{r} h_i(\mu)\{C_i x(t) + D_i(u(t) + g(x,t))\}. \tag{9}$$

This subsection proposes a terminal sliding surface for the TSFM given in (7) and (8). Consider the following terminal sliding surface:

$$\sigma = \dot{x}_1 + s x_1^{q/\beta} = x_2 + s x_1^{q/\beta}, \tag{10}$$

where the matrix $s = \sum_{i=1}^{r} h_i(\mu)s_i > 0$ denotes the nonlinear sliding surface gain with the appropriate dimension to be designed. Also, $q > 0, \beta > 0$ are integer odd numbers, and $2q > \beta > q$.

Lemma 1. *The reduced-order sliding mode dynamics surface (10) for control the T-S fuzzy model (7) and (8) can be reached through the following control input.*

$$u(t) = \sum_{i=1}^{r} h_i(z)\left(\mathrm{MB}_{1s,i}\right)^{-1} M\left(\left(-A_{s,i}x(t) - \rho sign(\sigma) - s\sigma_e + \varphi\sigma\right)\right), \tag{11}$$

where $\sigma_e = (q/\beta)\dot{x}_1 {x_1}^{(q/\beta-1)}$; is infinitely stable and M is a non-zero arbitrary matrix of appropriate dimension such that $MB_{(1s,i)}$ becomes an invertible matrix. Similarly, is a scalar matrix of appropriate dimension such that $Real(\varphi) < 0$.

Proof. Select a Lyapunov candidate function as follows:

$$V = \sigma^T\sigma, \tag{12}$$

where the time derivative of the sliding surface (10) is

$$\dot{\sigma} = x_1 + s\left(\frac{q}{\beta}\right){x_1}^{q/\beta-1}\dot{x}_1. \tag{13}$$

Now, applying time derivation to the Lyapunov function (12) leads to

$$\begin{aligned}\dot{V} = \sigma^T\dot{\sigma} + \dot{\sigma}^T\sigma &= \left(\dot{x}_1 + s{x_1}^{q/\beta}\right)^T\left(x_1 + s\frac{q}{\beta}\dot{x}_1{x_1}^{q/\beta-1}\right)\\ &+ \left(x_1 + s\left(\frac{q}{\beta}\right)\dot{x}_1{x_1}^{q/\beta-1}\right)^T\left(\dot{x}_1 + s{x_1}^{q/\beta}\right).\end{aligned} \tag{14}$$

Then, by definition of $\sigma_e = (q/\beta)\dot{x}_1{x_1}^{q/\beta-1}$, (14) is rewritten as

$$\dot{V} = \sigma^T\left(\sum_{i=1}^{r} h_i(\mu)\left\{A_{s,i}x(t) + B_{1s,i}(u(t) + g(x,t)) + s\sigma_e\right\}\right) + (*). \tag{15}$$

Let $A_s = \sum_{i=1}^{r} h_i(\mu)A_{s,i}$, $B_{1s} = \sum_{i=1}^{r} h_i(\mu)B_{1s,i}$. Then, the system state dynamics (7) and (8) and the time derivative of the Lyapunov function (15) are rewritten as

$$\begin{aligned}\dot{x}_1(t) &= x_2(t),\\ \dot{x}_2(t) &= A_s x(t) + B_{1s}(u(t) + g(x,t)),\\ \dot{V} &= \sigma^T\left(A_s x(t)\right) + B_{1s}\left(u(t) + g\left((x,t) + s\sigma_e\right)\right) + (*).\end{aligned} \tag{16}$$

Now, suppose that the Euclidean norm of the $B_{1s}g(x,u,t)$ is bounded by a known function $\rho(x,u,t)$, i.e., $\|\sum_{i=1}^{r} h_i(\mu)B_{1s,i}g(x,u,t)\| \le \rho$, where $\rho > 0$ is a known scalar value. Hence, substituting (11) in (16) yields

$$\begin{aligned}\dot{V} &= \sigma^T\left(-\rho\mathrm{sign}(\sigma) + B_{1s,i}g(x,t)\right)\\ &+ \sigma^T\varphi\sigma + \left(-\rho\mathrm{sign}(\sigma) + B_{1s,i}g(x,t)\right)^T\sigma + \varphi\sigma^T\sigma,\end{aligned} \tag{17}$$

where (17) according to uncertainty upper-bound $\rho(x,u,t)$ can be rewritten as

$$\begin{aligned}\dot{V} &= \left(-\rho \mid \sigma^T \mid + \sigma^T B_{1s,i} g(x,t) + \sigma^T \varphi\sigma\right) + (*) \le \left(-\rho\|\sigma\|_2 + \sigma^T B_{1s,i} g(x,t) + \varphi\sigma^T\sigma\right) \\ &\quad + (*) \le \left(-\rho\|\sigma\|_2 + \|\sigma\|_2 \mid B_{1s,i} g(x,t) \mid + \varphi\sigma^T\sigma\right) + (*) \le 0.\end{aligned} \tag{18}$$

Therefore, from (18), one can conclude

$$\dot{V} \le 2\varphi\|\sigma\|^2 \le 0, \tag{19}$$

where φ is a matrix with a negative real part value; then reachability conditions are held and the proof is complete.

The uncertainty upper-bound ρ can be simplified by supposing $\rho = \epsilon + \delta\|x(t)\|$, where ϵ is a known small positive scalar value. In this paper, we suppose that the uncertainty bound is unknown and we should estimate the uncertainty bound, i.e., $\hat{\rho}$. Therefore, the proposed terminal sliding mode control input (11) can be rewritten as

$$u(t) = \left(\mathrm{MB}_{1s,i}\right)^{-1} M\left(-A_s x(t) - s\sigma_e + \varphi\sigma - \hat{\rho}\,\mathrm{sign}(\sigma)\right). \tag{20}$$

Let $\tilde{\delta} = \hat{\delta} - \delta$ be the difference between the estimated and real values of the upper-bound parameter δ. Then, the estimated uncertainty bound and its parameter are obtained as follows:

$$\hat{\rho} = \epsilon + \hat{\delta}\|x(t)\| \dot{\hat{\delta}} = \eta\|\sigma\|\|x(t)\|, \tag{21}$$

where η is a known small positive constant. □

3.1.1. Attention. According to the above explanations, the Lyapunov function has been chosen as a function of the delta sliding surface that first satisfies the above conditions; secondly, the Lyapunov function and then the sliding surface and then the first and second state variables converge to zero, which makes the system stable.

Lemma 2. *The sliding surface described in (10) converges in a finite amount of time when the state trajectories in (7) and (8) are combined with the control input (20), the estimated bound of matched uncertainty, and the parameter updating rule (21).*

Proof. we select a candidate Lyapunov functions as follows:

$$V_1 = \frac{1}{2}(\sigma)^T(\sigma) + \frac{1}{2\eta}(\tilde{\delta})^2. \tag{22}$$

Now, applying the time derivative to (22) yields

$$\begin{aligned}\dot{V}_1 &= \sigma^T\dot{\sigma} + \frac{1}{\eta}\tilde{\delta}\dot{\tilde{\delta}} = -\dot{\rho}|\sigma| + \sigma^T B_{1s,i} g(x,t) + \varphi\sigma^T\sigma + \frac{1}{\eta}\tilde{\delta}\dot{\tilde{\delta}} \le -\dot{\rho}|\sigma| + \sigma^T B_{1s,i} g(x,t) \\ &\quad + \varphi \mid \sigma^T\sigma \mid + \frac{1}{\eta}\tilde{\delta}\dot{\tilde{\delta}} \le -\dot{\rho}|\sigma| + \mid \sigma^T \mid \mid B_{1s,i} g(x,t) \mid + \varphi \mid \sigma^T\sigma \mid + \frac{1}{\eta}\tilde{\delta}\dot{\tilde{\delta}} \le -\dot{\rho}|\sigma| + \rho|\sigma| \\ &\quad + \varphi\|\sigma\|^2 + \frac{1}{\eta}\tilde{\delta}\dot{\tilde{\delta}} \le -\dot{\rho}\|\sigma\| + \rho\|\sigma\| + \varphi\|\sigma\|^2 + \frac{1}{\eta}\tilde{\delta}\dot{\tilde{\delta}} \\ &= \varphi\|\sigma\|^2 - (\dot{\delta} - \delta)\|x(t)\|\|\sigma\| + \frac{1}{\eta}\tilde{\delta}\dot{\tilde{\delta}}.\end{aligned} \tag{23}$$

Substituting $\dot{\hat{\delta}}$ given in (20) in (22) yields

$$\dot{V}_1 = \varphi\|\sigma\|^2 \le 0, \tag{24}$$

where the reachability condition is held and the proof is complete.

The TSFM (7) and (8) and the control input (20) must now be revised and represented in new form in order to achieve the optimal state feedback gain (25). To accomplish this, take into account the following representation for the entire TSFM with actuator uncertainty.

$$\begin{aligned}\dot{x}(t) &= \sum_{i=1}^{r} h_i(\mu)\left\{A_i x(t) + B_{1,i}(u(t) + g(x,t))\right\}, \\ z(t) &= \sum_{i=1}^{r} h_i(\mu)\left\{C_i x(t) + D_i(u(t) + g(x,t))\right\},\end{aligned} \tag{25}$$

where $A_i \in \mathbb{R}^{n\times n}$, $B_{1,i} \in \mathbb{R}^{n\times q}$, and $B_{2,i} \in \mathbb{R}^{n\times m}$ are the appropriate dimension matrices. The strict feedback form T-S fuzzy model in (7) and (8) can be proven equivalent to the TSFM proposed in (25) by introducing the parameter-varying matrices as follows:

$$A_{s,i} = \begin{bmatrix} \alpha_{21,i} & \alpha_{22,i} \end{bmatrix},$$
$$A_i = \begin{bmatrix} \alpha_{11,i} & \alpha_{12,i} \\ \alpha_{21,i} & \alpha_{22,i} \end{bmatrix}, \tag{26}$$

where

$$A_i = \begin{bmatrix} 0_{n_1 \times m} & I_{n_2 \times m} \\ \alpha_{21,i} & \alpha_{22,i} \end{bmatrix},$$
$$B_{1,i} = \begin{bmatrix} 0_{n_1 \times m} \\ B_{1s,i} \end{bmatrix}; \tag{27}$$
$$B_{2,i} = \begin{bmatrix} 0_{n_1 \times q} \\ B_{2s,i} \end{bmatrix}.$$

For the sake of simplicity, let

$$A_s = \sum_{i=1}^{r} h_i(\mu) A_{s,i},$$
$$A = \sum_{i=1}^{r} h_i(\mu) A_i,$$
$$B_1 = \sum_{i=1}^{r} h_i(\mu) B_{1,i}, \tag{28}$$
$$B_2 = \sum_{i=1}^{r} h_i(\mu) B_{2,i},$$

where the overall matrices in (28) are as follows:

$$A_s = \begin{bmatrix} \alpha_{21} & \alpha_{22} \end{bmatrix};$$
$$A = \begin{bmatrix} \alpha_{11} & \alpha_{12} \\ \alpha_{21} & \alpha_{22} \end{bmatrix};$$
$$B_1 = \begin{bmatrix} 0_{n_1 \times m} \\ B_{1s} \end{bmatrix}; \tag{29}$$
$$B_2 = \begin{bmatrix} 0_{n_1 \times q} \\ B_{2s} \end{bmatrix}.$$

The control input (20) can be recast by taking into account the reformulated parameters stated in (29), as follows:

$$\begin{aligned} u(t) &= (\mathrm{MB}_{1s})^{-1} M\left(-A_s x(t) - \rho \mathrm{sign}(\sigma) - s\sigma_e + \varphi\sigma\right) \\ &= (\mathrm{MB}_{1s})^{-1} M\left(-\alpha_{21} x_1 - \alpha_{22} x_2 + \varphi x_2 + \varphi s x_1^{q/\beta} - \rho \mathrm{sign}(\sigma) - s\sigma_e\right) \\ &= (\mathrm{MB}_{1s})^{-1} M\left(\begin{bmatrix} -\alpha_{21} & (\varphi I - \alpha_{22}) \end{bmatrix} x + \varphi s x_1^{q/\beta} - \rho \mathrm{sign}(\sigma) - s\sigma_e\right) \\ &= (\mathrm{MB}_{1s})^{-1} M\left(\begin{bmatrix} 0 & I \end{bmatrix} A_\lambda x - \varphi s x_1^{q/\beta} - \rho \mathrm{sign}(\sigma) - s\sigma_e\right), \end{aligned} \tag{30}$$

where $A_\lambda = \varphi I_{n\times n} - A$. Therefore, the control input can be rewritten as

$$\begin{aligned} u(t) &= u_{re}(t) + u_n(t), \\ u_{re}(t) &= (\mathrm{MB}_{1s})^{-1} M\left(\begin{bmatrix} 0 & I \end{bmatrix} A_\lambda x - \varphi s x_1^{q/\beta} - s\sigma_e\right), \\ u_n(t) &= -MB_{1s})^{-1} M\rho \mathrm{sign}(\sigma), \end{aligned} \tag{31}$$

where $u_{\mathrm{re}}(t)$ and $u_n(t)$ stand for the equivalent and switching control inputs. Section 3.2 delves into how Generalized Partial Eigenstructure Assignment optimizes sliding gain, driven by factors discussed earlier. These include using the Takagi–Sugeno (T-S) fuzzy model to handle uncertain nonlinearities, integrating it with sliding mode control for robustness and wider use, using adaptive methods for uncertainties linked to actuator dynamics, employing Terminal Sliding Mode Control (TSMC) to swiftly guide system dynamics to the sliding surface with robustness, recognizing the effectiveness of eigenstructure assignment for rapid control responses, and exploring the combination of adaptive uncertainty estimation with optimal TSMC. This method adjusts sliding surface gain dynamically for better responsiveness. Additionally, Section 3.3 expands to address output tracking in strict feedback nonlinear systems through the T-S fuzzy model. The main goal is to enhance control robustness, adaptability, and performance in complex and uncertain system dynamics. □

3.2. Optimal Sliding Gain Design Using Generalized Partial Eigenstructure Assignment. In the second step of the ideal TSMC design, we set $g(\bullet) = 0$ and $u_n(t) = 0$ and then assume that the TSM controller (30) only contains the equivalent control part, which corresponds to the control law (31), to demonstrate the disturbance attenuation/rejection property of the suggested approach for the nonlinear T-S fuzzy model (3). The system dynamics (3) is therefore revised as follows.

$$\begin{aligned}\dot{x}(t) &= \sum_{i=1}^{r} h_i(\mu)\left\{A_i x(t) + B_{1,i}u(t) + B_{2,i}w(t)\right\},\\ z(t) &= \sum_{i=1}^{r} h_i(\mu)\{C_i x(t) + D_i u(t)\}.\end{aligned} \tag{32}$$

The core challenge pertains to the adaptive identification of the optimal nonlinear sliding surface coefficient, denoted as S, with the dual objectives of ensuring system stability and fulfilling the performance criteria of H_2 characterization. This challenge remains pertinent even within the constraints of motion governed by H_2 considerations. To effectively address this intricate challenge, the approach involves addressing a multichannel H_2 state-feedback predicament, aimed at judiciously selecting the most suitable state feedback control input. This selection holds significant influence over the subsequent design of the sliding matrix gain, S. The formulation of a H_2-centric sliding mode control strategy is predicated on the delineation of two pivotal steps:

Step 1. The amalgamation of the multichannel H_2 optimization problem with the generalized partial eigenstructure assignment technique takes precedence. This entails the derivation of a state feedback matrix, denoted as K, which serves to fulfill not only the multichannel H_2 constraints but also the nuanced requirement of situating the m poles of individual rule consequence subsystems at precisely predefined negative eigenvalues.

Step 2. The explicit determination of the sliding matrix gain, S, is contingent upon the state feedback outcomes gleaned from the preceding Step 1.

The subsequent sections undertake a comprehensive exegesis of these critical steps, elucidating their intricacies and implications in depth.

3.2.1. $\mathbf{H_2}$*-LMI Characterization.* This subsection presents a new extended LMI characterization of H_2 performance for the TSFM (32) from disturbance input w to output z.

Lemma 3. *The following claims are identical for the nonlinear system (32):*

(a) $\exists K_j, j, i = 1, \ldots, r$, *such that* $A_i + B_{1,i}K_j$ *is a stable matrix and the* H_2 *performance specification from the disturbance input* w *to the output* z *is less than* γ.

(b) $\exists X > 0$ *and* $Z > 0$ *such that*

$$\sum_{i=1}^{r}\sum_{j=1}^{r} h_i h_j \begin{bmatrix} A_i X + B_{1,i}Y_j + X A_i^T + Y_j^T B_{1,i}^T & * \\ B_{2,i}^T X & -\gamma I \end{bmatrix} < 0, \tag{33}$$

$$\sum_{i=1}^{r}\sum_{j=1}^{r} h_i h_j \left(\begin{bmatrix} X & \left(C_i X + D_i Y_j\right)^T \\ C_i X + D_i Y_j & Z \end{bmatrix} \right) > 0, \tag{34}$$

$$\operatorname{trace}(Z) < 1, \tag{35}$$

where $Y_j = K_j X$.

(c) $\exists X > 0$, $Z > 0$ *and nonsingular matrix* G_j *such that for* $i, j = 1, \ldots, r$

$$\begin{bmatrix} -\left(G_j + G_j^T\right) & * & * \\ A_i G_j + B_{1,i}Y_j + X + G_j & -2X & * \\ B_{2,i}^T G_j & 0 & -\gamma I \end{bmatrix} < 0, \tag{36}$$

$$\begin{bmatrix} -\left(G_j + G_j^T\right) & * & * \\ X & -X & 0 \\ \left(C_i G_j + D_i Y_j\right) & 0 & -Z \end{bmatrix} < 0, \tag{37}$$

$$\operatorname{trace}(Z) < 1, \tag{38}$$

where $Y_j = K_j G_j$.

Proof. It should be noted that (a) and (b) are equivalent versions of the conventional H_2-state-feedback synthesis for the T-S fuzzy system proposed by Lemma (1) in [42]. Schur complement lemma allows for the rewriting of (36) as

$$\begin{bmatrix} \left\{ \begin{matrix} -\left(G_j + G_j^{\mathrm{T}}\right) + \\ \gamma^{-1}\left(B_{2,i}^T G_j\right)^{\mathrm{T}}\left(B_{2,i}^T G_j\right) \end{matrix} \right\} & * \\ \mathrm{A_i}G_j + \mathrm{B_{1,i}}Y_j + X + G_j & -2X \end{bmatrix} < 0, \tag{39}$$

in which $G_j + G_j^T > 0$. Applying the congruence transformation $\begin{bmatrix} G_j^{-T} & 0 \\ 0 & X^{-1} \end{bmatrix}$ on (39) results in

$$\begin{bmatrix} -\left(\widetilde{G}_j + \widetilde{G}_j^T\right) + \gamma^{-1}\left(B_{2,i}B_{2,i}^T\right) & * \\ \widetilde{X}\left(A_i + B_{1,i}K_{\mathrm{j}}\right) + \widetilde{X} + \widetilde{G}_j & -2\widetilde{X} \end{bmatrix} < 0, \tag{40}$$

where $\widetilde{G}_j = {G_j}^{-1}$, $\widetilde{X} = X^{-1}$, and $K_{\mathrm{j}} = Y_j {G_j}^{-1}$. Then, (40) can be rewritten as

$$\begin{bmatrix} \gamma^{-1}\left(B_{2,i}B_{2,i}^T\right) & * \\ \widetilde{X}\left(A_i + B_{1,i}K_j\right) + \widetilde{X} & -2\widetilde{X} \end{bmatrix} + \mathrm{herm}\left(\begin{bmatrix} -I \\ I \end{bmatrix}\widetilde{G}_{\mathrm{ij}}^T\begin{bmatrix} I & 0 \end{bmatrix}\right) < 0. \tag{41}$$

By using the Projection lemma [37], inequality (41) holds if the following inequalities are satisfied:

$$\begin{bmatrix} I \\ I \end{bmatrix}^T \begin{bmatrix} \gamma^{-1}\left(B_{2,i}B_{2,i}^T\right) & * \\ \widetilde{X}\left(A_i + B_{1,i}K_j\right) + \widetilde{X} & -2\widetilde{X} \end{bmatrix} \begin{bmatrix} I \\ I \end{bmatrix} < 0, \tag{42}$$

$$\begin{bmatrix} 0 \\ I \end{bmatrix}^T \begin{bmatrix} \gamma^{-1}\left(B_{2,i}B_{2,i}^T\right) & * \\ \widetilde{X}\left(A_i + B_{1,i}K_j\right) + \widetilde{X} & -2\widetilde{X} \end{bmatrix} \begin{bmatrix} 0 \\ I \end{bmatrix} < 0. \tag{43}$$

Inequality (42) indicates $\widetilde{X} < 0$ and inequality (43) is equivalent to

$$\widetilde{X}\left(A_i + B_{1,i}K_j\right) + \left(A_i + B_{1,i}K_{\mathrm{j}}\right)^T \widetilde{X}^T + \gamma^{-1}\left(B_{2,i}B_{2,i}^T\right) < 0. \tag{44}$$

By multiplying both sides of (44) by $X = \widetilde{X}^{-1}$, one obtains

$$A_i X + B_{1,i}Y_j + \left(A_i X + B_{1,i}Y_j\right)^T + \gamma^{-1}\left(X B_{2,i}{B_{2,i}}^T X\right) < 0, \tag{45}$$

where $Y_j = K_{\mathrm{j}}X$. From the Schur complement, (45) is equivalent to (33). The proof is completed. □

Note that by using the Projection lemma, one can realize that (37) is an extension of (34), and the proof is omitted for brevity.

3.2.2. Multichannel-$\mathbf{H_2}$ State-Feedback Gain Design Using LMI Characterization. The state feedback gain in this subsection is designed to conform to the following performance categorization.

$$\begin{aligned} \text{minimize } \|T_{w_\psi z_\psi}\|_2 \text{ subject to } & \|T_{w_1 z_1}\|_2^2 < \gamma_1, \ldots, \|T_{w_{\psi-1} z_{\psi-1}}\|_2^2 < \gamma_{\psi-1}, \\ & \|T_{w_{\psi+1} z_{\psi+1}}\|_2^2 < \gamma_{\psi+1}, \ldots, \|T_{w_{\aleph} z_{\aleph}}\|_2^2 < \gamma_{\aleph}, \end{aligned} \tag{46}$$

where L_ψ and R_ψ are weighted vectors used to select a specific input/output channel and T_{wz} represents a H_2 performance from w to the output vector z [43]. The number of channels is specified by $\aleph$. By replacing $B_{2,i}, C_i$, and D_i in (32) with $B_{2\psi,i}, C_{\psi,i}$, and $D_{\psi,i}$, respectively, where $\psi = 1, \ldots \aleph$, it is possible to derive $\|T_{w_\psi z_\psi}\|_2 \coloneqq \|L_\psi T_{wz} R_\psi\|_2$. By minimizing the H_2 norm, a specific H_2 performance associated with signals $\mathrm{w}_\psi = R_\psi \mathrm{w}$ and $z_\psi = L_\psi z$ can be ensured (46). Now, by recasting (36)–(38) with different Lyapunov variables $X_\psi > 0$ of ψ^{th} channel and global variables G_j, Y_j for all channels, the multichannel H_2 LMI characterization can be derived. Therefore, by using Lemma 3, the LMI characterization for the ψ th channel can be expressed as follows:

$$\begin{bmatrix} -\left(G_j + {G_j}^T\right) & * & * \\ A_i G_j + B_{1,i}Y_j + X_\psi + G_j & -2X_\psi & * \\ {B_{2,i}}^T G_j & 0 & -\gamma I \end{bmatrix} < 0, \tag{47}$$

$$\begin{bmatrix} -\left(G_j + {G_j}^T\right) & * & * \\ X & -X & 0 \\ \left(C_i G_j + D_i Y_j\right) & 0 & -Z \end{bmatrix} < 0, \tag{48}$$

$$\mathrm{trace}\,(Z) < 1, \tag{49}$$

where $X_\psi > 0, Z > 0$; G_j, and Y_j are global LMI decision variables and $Y_j = K_j G_j$ $(i, j = 1, \ldots, r)$. The optimization problem (46) is then modified to

$$\begin{aligned} &\text{minimize } \gamma_\psi \text{ subject to} \\ &(47) \text{ and } (48), \text{and } (49) \text{ for } \psi - \text{th channel}, \\ &(47) \text{ and } (48), \text{and } (49) \text{ for } \theta - \text{th channel}, \\ &\text{with given } \gamma_\theta;\ \theta \neq \psi; \theta = 1, \ldots, \aleph. \end{aligned} \tag{50}$$

3.2.3. Generalized Partial Eigenstructure Assignment. The LMI characterizations (47)–(49) can be utilized to assign the m poles of each rule consequence linear subsystem (27) to a set of predetermined negative values (51) utilizing the PDC controller. Assignments of partial eigenstructures, which combine H_2 performance, are suggested in this subsection. The assignment of the following partial eigenstructures is done by state feedback.

$$\overbrace{\{\lambda, \ldots, \lambda\}}^{m \text{ times}}, \tag{51}$$

This issue can be broken down into the following two steps.

(1) Calculate the base vector $\begin{bmatrix} M_{\lambda,j} & N_{\lambda,j} \end{bmatrix}^T$ in the null space $\begin{bmatrix} A_j - \lambda I & B_{1,j} \end{bmatrix}$ for j = $1, \ldots, r$.

(2) The state feedback can be calculated as $K_j = Y_j G_j^{-1}$ with arbitrary $\eta_1, \ldots, \eta_m \epsilon \mathbb{R}^m$

$$Y_j = N_j \Sigma_N, G_j = M_j \Sigma_M, \tag{52}$$

where

$$\begin{aligned} N_j &\coloneqq \left[\overbrace{N_{\lambda,j}, \ldots, N_{\lambda,j}}^{m \text{ times}}, \overbrace{I, \ldots, I}^{(n-m)\text{times}} \right], \\ M_j &\coloneqq \left[\overbrace{M_{\lambda,j}, \ldots, M_{\lambda,j}}^{m \text{ times}}, \overbrace{I, \ldots, I}^{(n-m)\text{times}} \right], \\ \Sigma_N &\coloneqq \operatorname{diag}[\eta_1, \ldots, \eta_m, k_1, \ldots, k_{n-m}], \\ \Sigma_M &\coloneqq \operatorname{diag}[\eta_1, \ldots, \eta_m, l_1, \ldots, l_{n-m}], \end{aligned} \tag{53}$$

such that $k_1, \ldots, k_{n-m} \epsilon \mathbb{R}^n$, and $l_1, \ldots, l_{n-m} \epsilon \mathbb{R}^n$. It should be noted that some Σ_N and Σ_M arrays are dependent on the assignment of m eigenstructure to a predetermined value λ. In other words, other arrays that are not used for eigenvalue assignment can be used to achieve additional constraints. As a result, the first step in designing a H_2-based SMC is to recast (50) by the LMI characterizations (47)–(49) with $X > 0$, $Z > 0$, $\Sigma_{N,j}, \Sigma_{M,j}$, and $\gamma_i > 0$ as shown below.

$$\begin{aligned} &\text{minimize } \gamma_\psi \\ &\text{subject to} \\ &(47), (48), (49) \text{ and } (52) \text{ for } \psi - \text{th channel}, \\ &(44), (45), (46) \text{ and } (52) \text{ for } \theta - \text{th channel}, \\ &\text{with given } \gamma_\theta;\ \theta \neq \psi; \theta = 1, \ldots, \aleph. \end{aligned} \tag{54}$$

Each local subsystem (2) with PDC controller (5) contain eigenvalues (51), if (52) be used to calculate state feedback, which is proved by the following lemma.

Lemma 4. *The set of eigenvalues $A_j + B_{1,j} k_j$ for each fuzzy rule with the state feedback $k_j = Y_j G_j^{-1}$, where Y_j and G_j are reported in (52), contains the subset (51) for each fuzzy rule.*

Proof. The following brief proof demonstrates that a set of (51) is the subset of eigenvalues $A_j + B_{1,j} k_j$.

$$\begin{aligned} \left(A_j + B_{1,j} K_j\right) M_{\lambda,j} \eta_i &= \left[A_j + B_{1,j} \left(N_j \Sigma_{N,j} \right) \left(M_j \Sigma_{M,j} \right)^{-1} \right] M_{\lambda,j} \eta_i \\ &= \left\{ \begin{array}{c} A_j + B_{1,j} \left(\left[N_{\lambda_{,j}}, \ldots \right] \operatorname{diag}[\eta_1, \ldots] \right) \\ \left(\left[M_{\lambda_{,j}}, \ldots \right] \operatorname{diag}[\eta_1, \ldots] \right)^{-1} \end{array} \right\} \left(\left[M_{\lambda_{,j}}, \ldots \right] \operatorname{diag}[\eta_1, \ldots] \right) e_i \\ &= A_j M_{\lambda,j} \eta_i + B_{1,j} N_{\lambda,j} \eta_i = \lambda M_{\lambda,j} \eta_i, \end{aligned} \tag{55}$$

where $i = 1, \ldots, m$, and e_i stands for the canonical or standard basis of $\mathbb{R}^n$ [44–47]. □

$$\left(\mathrm{MB}_{1s,i}\right)^{-1} M\left(\left[\, 0_{n_2 \times n_1} \;\; I_{n_2 \times n_1} \,\right] A_{\lambda,i} x - \varphi s_i x_1^{q/\beta} - s_i \sigma_e\right) = K_i x. \tag{56}$$

If $u_i(t) = K_i x$ is used as the state feedback control input, then (56) can be expressed as follows:

$$\left(\left[\, 0 \;\; I \,\right] A_{\lambda,i} x - \varphi s x_1^{q/\beta} - s_i \sigma_e\right) = B_{1s,i} K_i x. \tag{57}$$

Flowing minimization is suggested to resolve (57):

$$\begin{aligned} \left(\left[\, 0 \;\; I \,\right] A_{\lambda,i} x - \varphi s_i x_1^{q/\beta} - s_i \sigma_e\right) - B_{1s,i} K_i x \le \left| \left(\left[\, 0 \;\; I \,\right] A_{\lambda,i} x - \varphi s_i x_1^{q/\beta} - s_i \sigma_e\right) - B_{1s,i} K_i x \right| \\ \le \left\| \left(\left[\, 0 \;\; I \,\right] A_{\lambda,i} x - \varphi s_i x_1^{q/\beta} - s_i \sigma_e\right) - B_{1s,i} K_i x \right\| < \delta_i, \end{aligned} \tag{58}$$

where K_i is the state feedback gain, derived from (56), and $\delta_i > 0$ is the scalar variable. This ensures that the m poles of each rule consequence subsystem with PDC controller are precisely situated at λ [48–50].

By employing a straightforward relaxation procedure, one can analyze (58) and obtain the positive definite matrix s_i as shown below:

$$\begin{aligned} &\text{minimize } \delta_i \text{ subject to} \\ &\left\| \left[\, 0 \;\; I \,\right] A_{\lambda,i} x - \varphi s_i x_1^{q/\beta} - s_i \sigma_e - B_{1s,i} K_i x \right\| < \delta_i, \quad \text{for } i = 1, \ldots, r. \end{aligned} \tag{59}$$

Using LMI optimization, the minimization problem stated in (59) is reformulated as follows:

$$\begin{aligned} &\text{minimize } \delta_i \text{ subject to} \\ &\begin{bmatrix} -\delta_i I & * \\ \left[\, 0 \;\; I \,\right] A_{\lambda,i} x - \varphi s_i x_1^{q/\beta} - s_i \sigma_e - B_{1s,i} K_i x & -\delta_i I \end{bmatrix} < 0; \quad \text{for } i = 1, \ldots, r. \end{aligned} \tag{60}$$

As a result, the multichannel-H_2-based terminal SMC problem is summarised in (60) to find the global solution for the optimization problem, yielding the terminal sliding mode gain s [51, 52].

The following theorem offers a concise statement of the suggested design strategy for the multichannel H_2-based Adaptive Dynamic TSMC for (25) [53–55].

Theorem 5. *Assume that the state feedback K is a solution to the optimization problem (56) for some $\gamma_\psi > 0$, $\psi = 1, \ldots \aleph$. The multichannel H_2-performance constraints $\|T_{w_\psi \varnothing_\psi}\|_2^2 < \gamma_\psi$, $\psi = 1, \ldots \aleph$ are then guaranteed, and the resulting reduced-order sliding mode dynamics obtained by the control law are demonstrated as*

$$u(t) = \sum_{i=1}^{r} h_i(z(t)) k_i x(t) + u_n(t), \tag{61}$$

where $u_n(t)$ represents the switching control component of the proposed controller in (20), which is asymptotically stable.

Proof. Select a candidate Lyapunov function as follows:

$$V_2 = \frac{1}{2} x^T x. \tag{62}$$

3.2.4. Adaptive Sliding Gain Matrix Design. The fact that (6) equals (11) can lead to one approach for determining the sliding gain matrix, which proceeds as follows:

Using the time derivative to analyze the Lyapunov function (62) now results in

$$\dot{V}_2 = x^T \dot{x}, \tag{63}$$

and substituting $\dot{x}(t)$ from (25) in (63) yields

$$\dot{V}_2 = x^T \left(\sum_{i=1}^{r} h_i(\mu) \left\{ A_i x(t) + B_{1,i}(u(t) + g(x,t)) \right\} \right). \tag{64}$$

After that, (64) is revised as follows:

$$\dot{V}_2 = x^T \left(\sum_{i=1}^{r} h_i(\mu) \left\{ A_{s,i} x(t) + B_{1,i}(u(t) + g(x,t)) \right\} \right). \tag{65}$$

Substituting $u(t)$ from (61) into (65) yields

$$\begin{aligned} \dot{V}_2 &= x^T \left(\left\{ \sum_{i=1}^{r} \sum_{j=1}^{r} h_i h_j \left\{ \left(A_i + B_{1,i} K_j \right) x(t) + B_{1s,i} g(x,t) - \hat{\rho} \frac{\sigma}{\|\sigma\|} \right\} \right\} \right) \\ &\le x^T \left(\sum_{i=1}^{r} \sum_{j=1}^{r} h_i h_j \left\{ \left(A_i + B_{1,i} K_j \right) x(t) \right\} \right) \\ &\quad - \left(\left\{ \sum_{i=1}^{r} \sum_{j=1}^{r} h_i h_j \left\{ | x^T \hat{\rho} - x^T B_{1s,i} g(x,t) | \right\} \right\} \right) \le x^T \left(\sum_{i=1}^{r} \sum_{j=1}^{r} h_i h_j \left\{ \left(A_i + B_{1,i} K_j \right) x(t) \right\} \right) \\ &\quad - \epsilon \|x\|^2. \end{aligned} \tag{66}$$

In this study, it is claimed that $A_i + B_{1,i}K_j$ are Hurwitz matrices; hence, (66) leads to

$$\dot{V}_2 < \sum_{i=1}^{r} \sum_{j=1}^{r} h_i(\mu) h_j(\mu) \lambda_{\max,ij} \|x(t)\|^2 < 0, \tag{67}$$

where the reachability condition is satisfied, and the maximum eigenvalues of the Hurwitz matrices $A_i + B_{1,i}K_j$, i.e., $\lambda_{\max,ij}$, are located on the left side of the s-plane.

Hint 3.1. When the trajectories in this investigation are on the sliding surface, that is, when $\sigma = 0$, the system tracking dynamic is

$$\dot{e}_1 = -s e_1^{\,q/\beta}. \tag{68}$$

The real components of the e_1 eigenvalues are entirely negative, proving the infinite stability of the TSMC system. We can also rewrite (68) as

$$dt = -\frac{de}{s e_1^{\,q/\beta}}. \tag{69}$$

We now integrate both sides of (69). Then, using the closed interval $(e_1(0) \neq 0, e_1(t_s) = 0)$, we derive the resulting equation as follows:

$$t_s = -\frac{1}{s} \int_{e_1(0)}^{0} \frac{de}{e_1^{\,q/\beta}} = \frac{| e_1(0) |^{1-q/\beta}}{s(1 - q/\beta)}. \tag{70}$$

We can deduce from (70) that when the system with the initial condition $e_1(0) \neq 0$ arrives at the terminal sliding mode at $t = t_r$, the system state e_1 converges to $e_1(t_s) = 0$ in finite time and remains there for $\ge t_s$. In other words, for $t \ge t_r$, the state trajectory will belong to the sliding line. However, the convergence time, t_s, given in (70), is affected by the parameters q/β and s. □

3.3. Application to Output Tracking. The suggested method in this paper is expanded to handle the challenge of output tracking in nonlinear systems characterized by strict feedback structure, employing the T-S fuzzy model. The output to be measured is represented as $y(t) = x_1(t)$. The subsequent steps are recommended to achieve this objective.

Step 1. The first state tracking error can be expressed as $e_1 = y(t) - y_d(t) = x_1 - x_d$, where $y_d(t)$ and x_d stand for the desired output vector and desired first state vector, respectively. This is because the measured output vector $y(t)$ is an available output vector. The first and second time derivatives of e_1 are then calculated as shown below.

$$\begin{aligned} \dot{e}_1 &= \dot{x}_1 - \dot{x}_d = x_2 - \dot{x}_d, \\ \ddot{e}_1 &= \ddot{x}_1 - \ddot{x}_d = \dot{x}_2 - \ddot{x}_d \\ &= \sum_{i=1}^{r} h_i(\mu) \left\{ A_{s,i} x(t) + B_{1s,i}(u(t) + g(x,t)) \right\} - \ddot{x}_d. \end{aligned} \tag{71}$$

Define $e_2 = \dot{e}_1$, and the system tracking error dynamics (8) is rewritten as

$$\begin{aligned}\dot{e}_1 &= e_2,\\ \dot{e}_2 &= \sum_{i=1}^{r} h_i(\mu)\left\{A_{s,i}x(t) + B_{1s,i}(u(t) + g(x,t))\right\} - \ddot{x}_d.\end{aligned} \tag{72}$$

The output tracking problem (72), which is now expressed in terms of the tracking error $e(t) = \begin{bmatrix} e_1 & e_2 \end{bmatrix}^T$ and time-derivative of the tracking error $\dot{e}(t) = \begin{bmatrix} \dot{e}_1 & \dot{e}_2 \end{bmatrix}^T$, is to be developed with a new control input $\tau(t)$. This equation must be true for the new control input:

$$\sum_{i=1}^{r} h_i B_{1s,i}\tau(t) \triangleq \sum_{i=1}^{r} h_i B_{1s,i}u(t) + \sum_{i=1}^{r} h_i A_{s,i}x_d(t) - \ddot{x}_d(t). \tag{73}$$

Then, system (72) is rewritten as

$$\begin{aligned}\dot{e}_1 &= e_2,\\ \dot{e}_2 &= \sum_{i=1}^{r} h_i(\mu)\left\{A_{s,i}e(t) + B_{1s,i}(\tau(t) + g(x,t))\right\}.\end{aligned} \tag{74}$$

Now, the terminal sliding surface for the state tracking error (74) can be modified as

$$\sigma = \dot{e}_1 + se_1^{q/\beta} = \left(x_2 - \dot{x}_d\right) + se_1^{q/\beta}, \tag{75}$$

where the appropriate dimension matrix $s > 0$ stands for the nonlinear sliding surface gain. The new control input of the TSMC given in (75) can be proposed as

$$\begin{aligned}\tau(t) &= \tau_{re}(t) + \tau_n(t),\\ \tau_{\mathrm{re}}(t) &= \left(\mathrm{MB}_{1s,i}\right)^{-1} M\left(\begin{bmatrix} 0_{n_2\times n_1} & I_{n_2\times n_1}\end{bmatrix} A_\lambda e - \varphi \mathrm{se}_1^{\,q/\beta} - s\left(\frac{q}{\beta}\right)\dot{e}_1 e_1^{\,q/\beta-1}\right),\\ \tau_n(t) &= -\left(\mathrm{MB}_{1s,i}\right)^{-1} M\rho\,\mathrm{sign}(\sigma),\end{aligned} \tag{76}$$

where $\tau_{\mathrm{re}}(t)$ and $\tau_n(t)$ denote the equivalent and switching new control input, respectively.

Step 2. In this case, assuming that $D_i|_{i=1,..,r} = 0$, we define the H_2-performance output tracking error as $z(t) = z(t) - z_d(t)$, where $z_d(t)$ represents the desired H_2-performance output vector. The output tracking error dynamics is then changed as (77) to evaluate the disturbance attenuation supplied for the system dynamic given in (32).

$$\begin{aligned}\dot{e}(t) &= \sum_{i=1}^{r} h_i(\mu)\left\{A_i e(t) + B_{1,i}\tau(t) + B_{2,i}w(t)\right\},\\ \tilde{z}(t) &= \sum_{i=1}^{r} h_i(\mu)\{C_i e(t)\}.\end{aligned} \tag{77}$$

According to the PDC form, the new control input $\tau(t)$ is now designed for the tracking error dynamic (77) as

$$\tau(t) = \sum_{i=1}^{r} h_i(\mu(t))\mathfrak{K}_i\tilde{x}(t), \tag{78}$$

such that the new control input gains in (78) are acquired by solving the optimization problem (56).

Step 3. For the output tracking problem, the terminal sliding mode gain s must be obtained. As a result of (77) and (78), the minimization problem (60) is modified accordingly in this case.

minimize δ_i subject to

$$\begin{bmatrix} -\delta_i I & * \\ \begin{bmatrix} 0 & I\end{bmatrix} A_{\lambda i}e + \varphi s_i e_1^{q/\beta} + s_i\left(\frac{q}{\beta}\right)\dot{e}_1 e_1^{(q/\beta)-1} - B_{1s,i}K_i e & -\delta_i I \end{bmatrix} < 0, \quad \text{for } i = 1,\ldots,r. \tag{79}$$

Step 4. The sliding surface gain S obtained in the optimization problem (79) and the new control input condition given in (76) are used to calculate the practical control input $u(t)$.

4. Simulation Results

In this section, a real-world illustration involving a mass-spring mechanical system is examined to evaluate the effectiveness and practicality of the suggested optimal adaptive terminal sliding mode control system design.

Example 1. Consider a mass-spring mechanical system depicted in Figure 1, where (x_1, x_2), (F_{f_1}, F_{f_2}), (F_{s_1}, F_{s_2}), (F_{μ_1}, F_{μ_2}), (m_1, m_2), and u denote the displacement from the reference points, the viscous damping forces, the restoring forces of the springs, the kinetic friction forces, the masses, and the external input, respectively. Newton's law states that the motion equations can be represented as

$$\begin{aligned} &m_1(\ddot{x}_1 - \ddot{x}_2) + k\left(1 + ka^2(x_1 - x_2)^2\right)(x_1 - x_2) + c(\dot{x}_1 - \dot{x}_2) \\ &\quad = u_1(t) + g(x) - w_1(t), \\ &m_2\ddot{x}_2 - c(\dot{x}_1 - \dot{x}_2) - k\left(1 + ka^2(x_1 - x_2)^2\right)(x_1 - x_2) + c\dot{x}_2 \\ &\qquad + k\left(1 + ka^2x_2^2\right)x_2 \\ &\quad = u_2(t) + g(x) - w_2(t), \end{aligned} \tag{80}$$

where the actuator uncertainty $(g(x))$ and the external disturbance $(w(t))$ are denoted correspondingly. The viscous damping force and the restoring force of the spring are both described by the variables $m_1 = m_2$, $c > 0$, k, and a^2 as $F_f = c\dot{x}$ and $F_s = k(1 + a^2)x^2$, respectively. The nonlinear system (80) is represented as the following state-space form by the definitions $X_1 = x_1 - x_2$, $X_2 = \dot{X}_1$, $X_3 = x_2$, and $X_4 = \dot{X}_3$.

$$\begin{aligned} \begin{bmatrix} \dot{X}_1 \\ \dot{X}_2 \\ \dot{X}_3 \\ \dot{X}_4 \end{bmatrix} &= \begin{bmatrix} 0 & 1 & 0 & 0 \\ -k - ka^2X_1^2 & -c & 0 & 0 \\ 0 & 0 & 0 & 1 \\ k + ka^2X_1^2 & c & -k - ka^2X_3^2 & -c \end{bmatrix} \begin{bmatrix} X_1 \\ X_2 \\ X_3 \\ X_4 \end{bmatrix} \\ &\quad + \begin{bmatrix} 0 & 0 \\ 1 & 0 \\ 0 & 0 \\ 0 & 1 \end{bmatrix} (u(t) + g(x)) + \begin{bmatrix} 0 \\ -1 \\ 0 \\ -1 \end{bmatrix} w(t), \\ y(t) &= \begin{bmatrix} 1 & 0 \\ 0 & 1 \end{bmatrix} \begin{bmatrix} X_1 \\ X_3 \end{bmatrix}, z_1(t) = X_1, z_2(t) = X_3. \end{aligned} \tag{81}$$

Using the sector nonlinearity approaches [1], we select X_1^2 and X_3^2 as the premise variables with the corresponding membership functions as $M_1(X_1^2) = (X_1^2 - \overline{d}_1)/(\overline{D}_1 - \overline{d}_1)$ and $M_2(X_1^2) = 1 - M_1(X_1^2)$, $N_1(X_3^2) = (X_3^2 - \overline{d})/(\overline{D}_3 - \overline{d}_3)$ and $N_2(X_3^2) = 1 - N_1(X_3^2)$, where $\overline{D}_1, \overline{D}_3$ and $\overline{d}_1, \overline{d}_3$ denote the upper and lower bounds of the premise variable, respectively. For the system dynamic (81), one derives the following desired state variable as

$$\begin{aligned} \left[X_{1d}(t) \;\; X_{3d}(t) \right]^T &= y_d(t), \left[X_{2d}(t) \;\; X_{4d}(t) \right]^T \\ &= \left[\dot{X}_{1d}(t) \;\; \dot{X}_{3d}(t) \right]^T. \end{aligned} \tag{82}$$

Therefore, one obtains the practical input from (71) and (81) as $u(t) = \tau(t) + cX_{2d} + (k + ka^2X_1^2)X_{1d}$. Here, the system parameters are set as $m_1 = m_2 = 1\text{kg}$, $c = 0.4$, $k = 1.1$, $a^2 = 0.9$. Also, $X_{1d} = \sin(0.2t)$ and $X_{3d} = 0.5\sin(0.2t)$ are selected as the desired output vector. Then, the upper and the lower bounds of the premise variables are obtained as $\overline{D}_1 = 1, \overline{D}_3 = 0.25$, and $\overline{d}_1 = \overline{d}_3 = 0$, respectively. The fuzzy rule matrices are obtained as

$$\begin{aligned} A_1 &= \begin{bmatrix} 0.00 & 1.00 & 0.000 & 0.00 \\ -2.09 & -0.40 & 0.000 & 0.00 \\ 0.00 & 0.00 & 0.000 & 1.00 \\ 2.09 & 0.40 & -1.595 & -0.4 \end{bmatrix}, \\ A_2 &= \begin{bmatrix} 0.00 & 1.00 & 0.000 & 0.00 \\ -1.10 & -0.40 & 0.000 & 0.00 \\ 0.00 & 0.00 & 0.000 & 1.00 \\ 1.10 & 0.40 & -1.595 & -0.40 \end{bmatrix}, \\ A_3 &= \begin{bmatrix} 0.00 & 1.00 & 0.000 & 0.00 \\ -2.09 & -0.40 & 0.000 & 0.00 \\ 0.00 & 0.00 & 0.000 & 1.00 \\ 2.09 & 0.40 & -1.100 & -0.40 \end{bmatrix}, \\ A_4 &= \begin{bmatrix} 0.00 & 1.00 & 0.000 & 0.00 \\ -1.10 & -0.40 & 0.000 & 0.00 \\ 0.00 & 0.00 & 0.000 & 1.00 \\ 1.10 & 0.40 & -1.100 & -0.4 \end{bmatrix}, \\ B_{1,1} &= \begin{bmatrix} 0 & 0 \\ 1 & 0 \\ 0 & 0 \\ 0 & 1 \end{bmatrix}, B_{2,1} = \begin{bmatrix} 0.0 \\ -1 \\ 0.0 \\ -1 \end{bmatrix}, \\ C_{1,1} &= \begin{bmatrix} 1 \\ 0 \\ 0 \\ 0 \end{bmatrix}^T, C_{2,1} = \begin{bmatrix} 0 \\ 0 \\ 1 \\ 0 \end{bmatrix}^T, \end{aligned} \tag{83}$$

and $B_{1,i} = B_{1,1}, B_{2,i} = B_{2,1}, C_{1,i} = C_{1,1}, C_{2,i} = C_{2,1}, D_{2,i} = D_{2,i} = \begin{bmatrix} 0 & 0 \end{bmatrix}$ $(i = 1, \ldots, 4)$.

In this study, we select the predetermined eigenvalue as $\lambda = -10$, the nonlinear sliding fractional power as $p/q = 7/9$, the initial state condition as $\begin{bmatrix} X_1 & X_2 & X_3 & X_4 \end{bmatrix}^T = \begin{bmatrix} 0 & 0.1 & 0 & 0.1 \end{bmatrix}^T$, the actuator uncertainty as $g(x) = \begin{bmatrix} 0.1X_1(t) & 0.1X_3(t) \end{bmatrix}^T$, and the arbitrary uncertainty parameters as $\epsilon = 1 \times 10^{-4}, \eta = 0.5$, and the external disturbance is as follows:

$$w(t) = 0.005 \sin(\pi X_1(t)), \quad \text{if } 0 \le X_1(t) \le \frac{1}{10}. \tag{84}$$

We devote different Lyapunov matrix variables for each channel in (51). Also, the predetermined value $\gamma_2 = 2.3638$ is considered for the H_2-performance from the external disturbance vector to the first H_2 output vector, i.e., $z_2(t)$. Then, the results show that the H_2-performance $\gamma_1 = 2.9776$ is obtained for the first H_2 output vector, i.e., $z_1(t)$. In this case, the state feedback gains and the optimal sliding gains are obtained as

$$\begin{aligned}
Y_1 &= \begin{bmatrix} 0.5634 & -5.6198 & -0.0017 & -0.2495 \\ 0.0336 & -0.5254 & 1.8202 & -2.8749 \end{bmatrix}, \\
Y_2 &= \begin{bmatrix} 0.5633 & -5.6198 & -0.0017 & -0.2495 \\ 0.0345 & -0.5254 & 1.8202 & -2.8749 \end{bmatrix}, \\
Y_3 &= \begin{bmatrix} 0.5634 & -5.6198 & -0.0017 & -0.2495 \\ 0.0336 & -0.5254 & 1.8202 & -2.8749 \end{bmatrix}, \\
Y_4 &= \begin{bmatrix} 0.5633 & -5.6198 & -0.0017 & -0.2495 \\ 0.0345 & -0.5254 & 1.8202 & -2.8749 \end{bmatrix}, \\
G_1 &= \begin{bmatrix} 0.0057 & 0.0637 & -0.0005 & 0.0019 \\ -0.0574 & 0.3854 & 0.0005 & -0.0011 \\ 0.0002 & 0.0020 & 0.7833 & 0.3983 \\ -0.0023 & 0.0043 & -1.0300 & 1.0571 \end{bmatrix}, \\
G_2 &= \begin{bmatrix} 0.0058 & 0.0637 & -0.0005 & 0.0019 \\ -0.0580 & 0.3854 & 0.0005 & -0.0011 \\ 0.0002 & 0.0020 & 0.7833 & 0.3983 \\ -0.0023 & 0.0043 & -1.0300 & 1.0571 \end{bmatrix}, \\
G_3 &= \begin{bmatrix} 0.0057 & 0.0637 & -0.0005 & 0.0019 \\ -0.0574 & 0.3854 & 0.0005 & -0.0011 \\ 0.0002 & 0.0020 & 0.7833 & 0.3983 \\ -0.0023 & 0.0043 & -1.0300 & 1.0571 \end{bmatrix}, \\
G_4 &= \begin{bmatrix} 0.0058 & 0.0637 & -0.0005 & 0.0019 \\ -0.0580 & 0.3854 & 0.0005 & -0.0011 \\ 0.0002 & 0.0020 & 0.7833 & 0.3983 \\ -0.0018 & 0.0043 & -1.0300 & 1.0571 \end{bmatrix}, \\
F_1 &= \begin{bmatrix} -18.0133 & -11.6054 & -0.1949 & -0.1428 \\ -3.1727 & -0.8082 & -0.8346 & -2.4005 \end{bmatrix}, \\
F_2 &= \begin{bmatrix} -18.3823 & -11.5444 & -0.1945 & -0.1423 \\ -3.0549 & -0.8276 & -0.8348 & -2.4007 \end{bmatrix}, \\
F_3 &= \begin{bmatrix} -18.0133 & -11.6053 & -0.1949 & -0.1428 \\ -3.1745 & -0.8079 & -0.8346 & -2.4005 \end{bmatrix}, \\
F_4 &= \begin{bmatrix} -18.3824 & -11.5444 & -0.1945 & -0.1423 \\ -3.0566 & -0.8274 & -0.8347 & -2.4007 \end{bmatrix}.
\end{aligned} \tag{85}$$

A standard TSMC based on T-S fuzzy model (81) and (82) combined with H_2 performance is analyzed in order to compare the proposed approach's effectiveness with that of similar efforts. This approach demonstrates that the H_2 performance $\gamma = 14.4588$ is assured. Figures 2–13 contain the illustrated comparative simulations.

$$\begin{aligned}
F_1 &= \begin{bmatrix} -0.8955 & -0.8822 & -0.0184 & 0.0020 \\ -2.1030 & -0.3899 & -1.3906 & -0.8823 \end{bmatrix}, \\
F_2 &= \begin{bmatrix} -1.8855 & -0.8822 & -0.0185 & 0.0020 \\ -1.1130 & -0.3899 & -1.3906 & -0.8823 \end{bmatrix}, \\
F_3 &= \begin{bmatrix} -0.8955 & -0.8822 & -0.0184 & 0.0020 \\ -2.1030 & -0.3899 & -1.8856 & -0.8823 \end{bmatrix}, \\
F_4 &= \begin{bmatrix} -1.8855 & -0.8822 & -0.0185 & 0.0020 \\ -1.1130 & -0.3899 & -1.8856 & -0.8823 \end{bmatrix}.
\end{aligned} \tag{86}$$

Figures 2–4 illustrate the superiority of the adaptive optimal TSMC approach over the conventional method with respect to reference tracking. In Figures 6 and 7, the trajectories of the first and second vectors on the surface demonstrate that the adaptive optimal TSMC approach reaches the origin point more rapidly and with minimal chattering compared to the conventional method. Figures 8 and 9 visualize the new control inputs proposed in (76), computed by integrating the H_2 characterization and the generalized eigenstructure assignment method through the adaptive optimal TSMC minimization problem (79) alongside the calculation using the conventional method. Figures 6–9 indicate that the method proposed in this paper offers numerous advantages, including a significant reduction in chattering phenomena and its adverse effects, decreased control effort, and notably reduced reaching time.

To demonstrate the effectiveness of the proposed approach in reducing reaching time and chattering phenomena, refer to Figures 10 and 11. Furthermore, according to (81) and Figure 1, the first H_2 output vector, $z_1(t)$, denotes the difference between the displacements of the first and second masses. It is preferable for these functions to reach zero in finite time with minimal chattering to ensure smooth displacement. On the other hand, the second H_2 output vector, $z_2(t)$, solely represents the displacement of the second mass. Figure 12 shows that $z_1(t)$ reaches zero faster than that with the conventional method. Figures 12 and 13 demonstrate that although the difference in the second mass displacement ($z_1(t)$) is not substantial using both approaches, the disparity in finding the displacement of the first mass ($e_1(t)$) between the two approaches is remarkable.

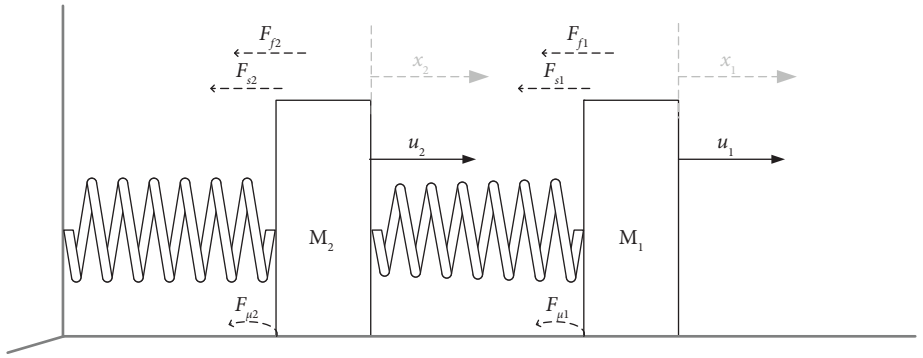

Figure 1: Mass-spring mechanical system.

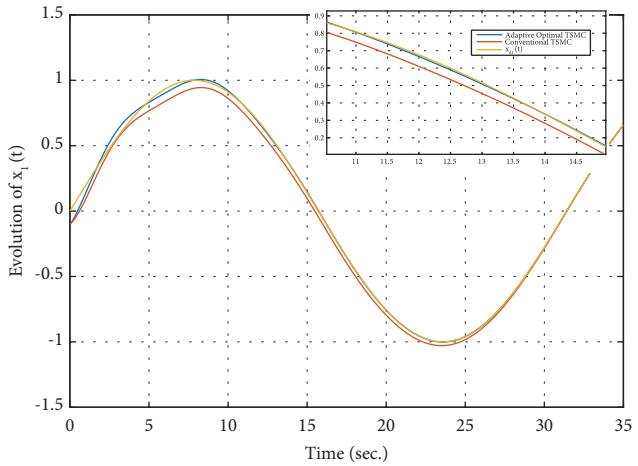

Figure 2: Responses of x_1 and x_{1d}.

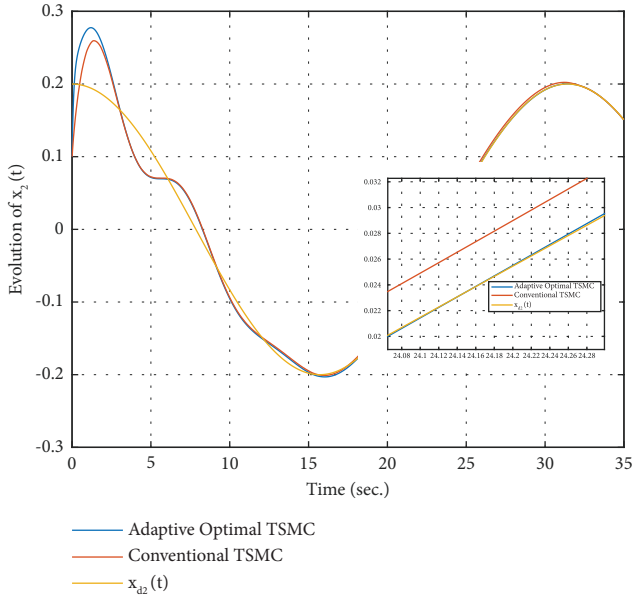

Figure 3: Responses of x_2 and x_{2d}.

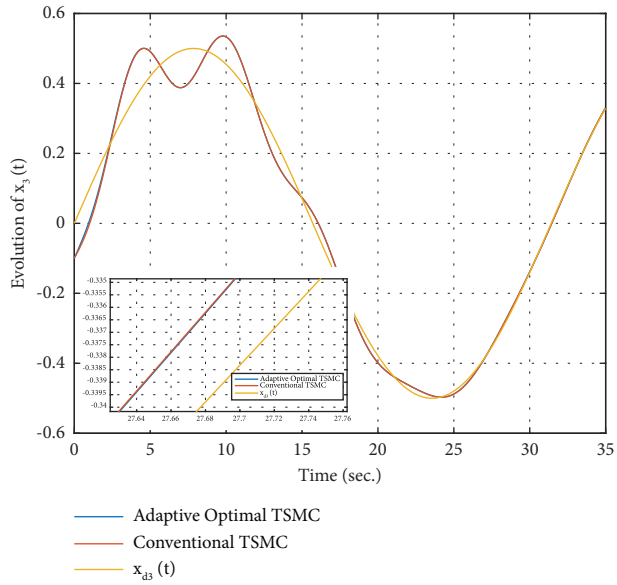

Figure 4: Responses of x_3 and x_{3d}.

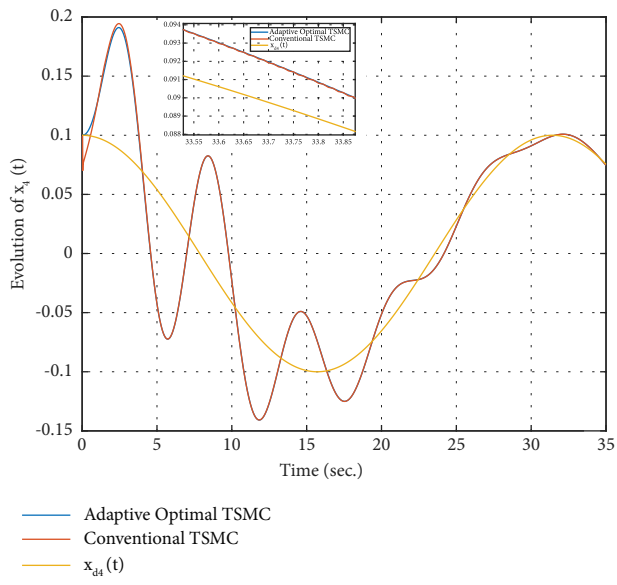

Figure 5: Responses of x_4 and x_{4d}.

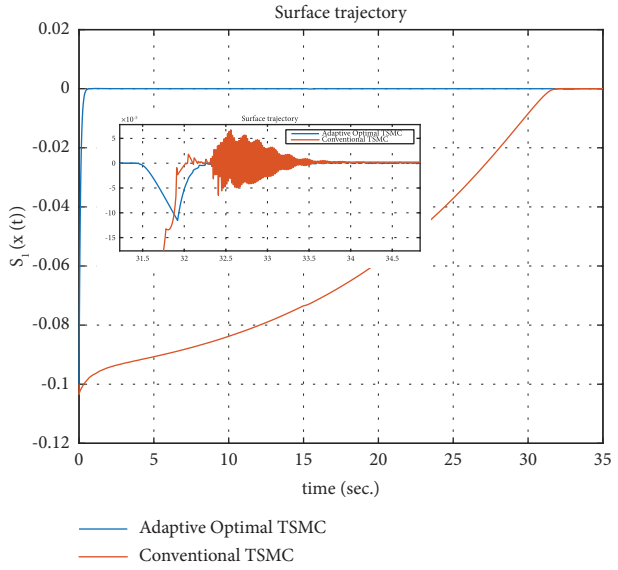

Figure 6: The evolution of the first vector of two-dimensional sliding surface vector.

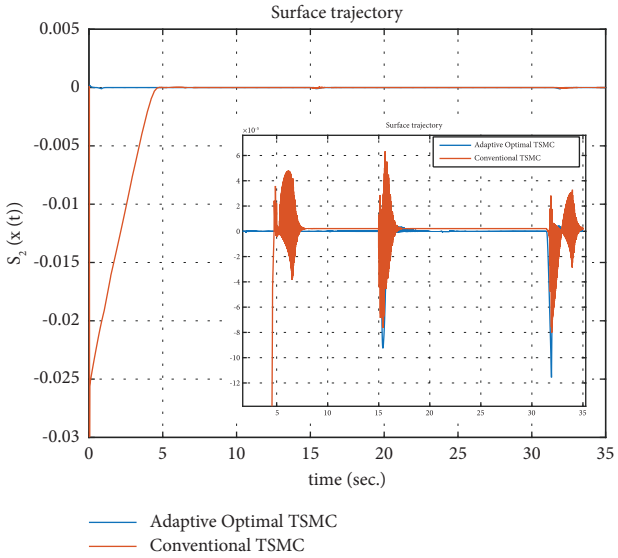

Figure 7: The evolution of the second vector of two-dimensional sliding surface vector.

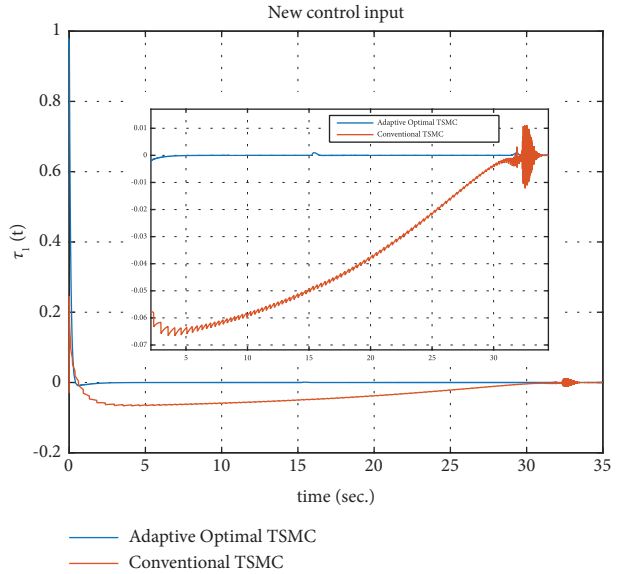

Figure 8: The first vector of the two-dimensional new control input signal vector $\tau(t)$.

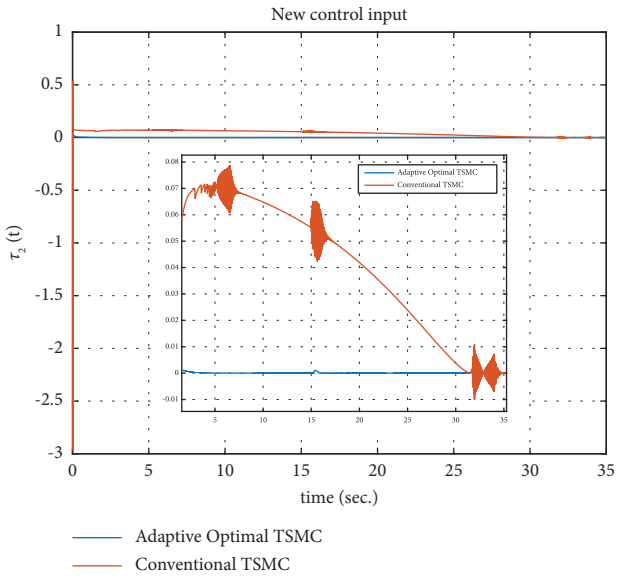

Figure 9: The second vector of the two-dimensional new control input signal vector $\tau(t)$.

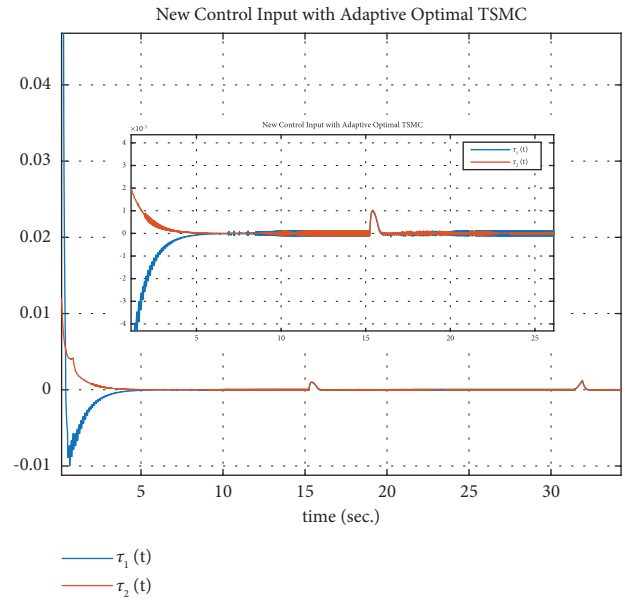

Figure 10: The trajectory of $\tau_1(t)$ and $\tau_2(t)$.

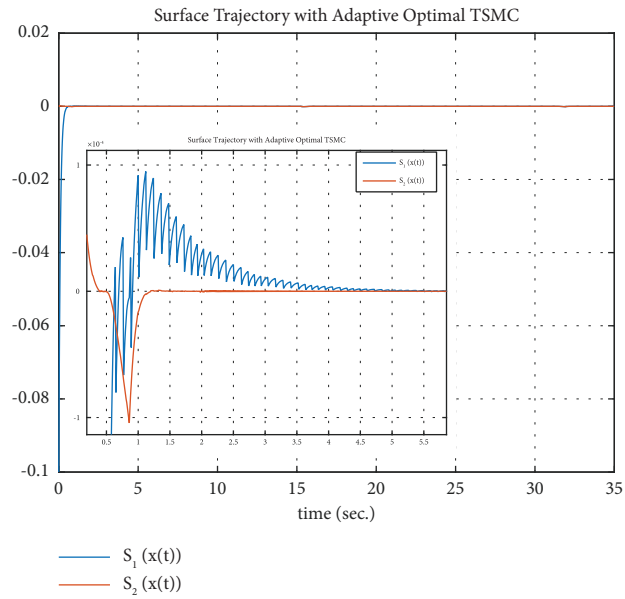

Figure 11: The trajectory of $s_1(t)$ and $s_2(t)$.

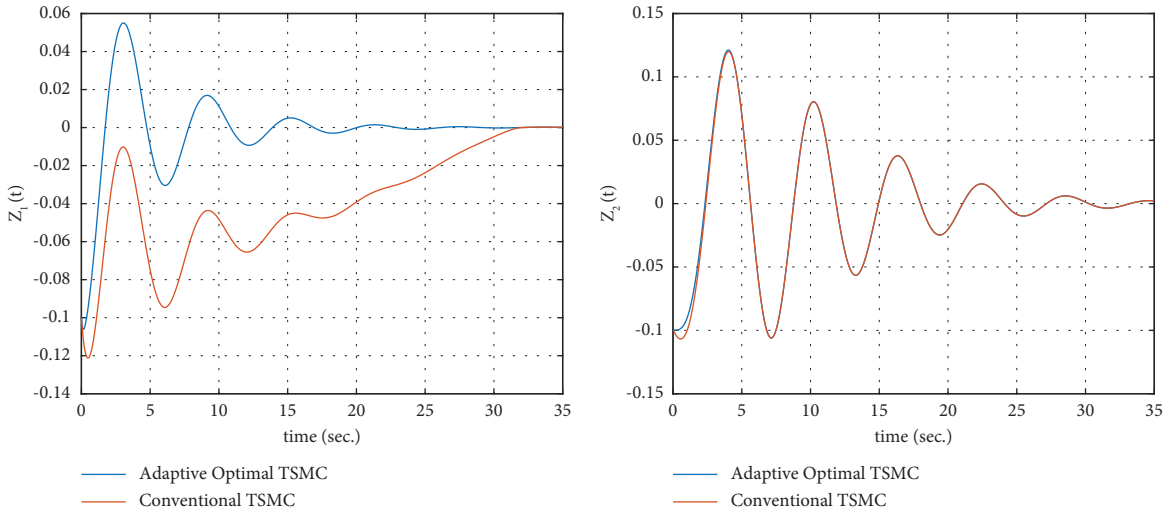

FIGURE 12: The trajectory of (a) $z_1(t)$ and (b) $z_2(t)$.

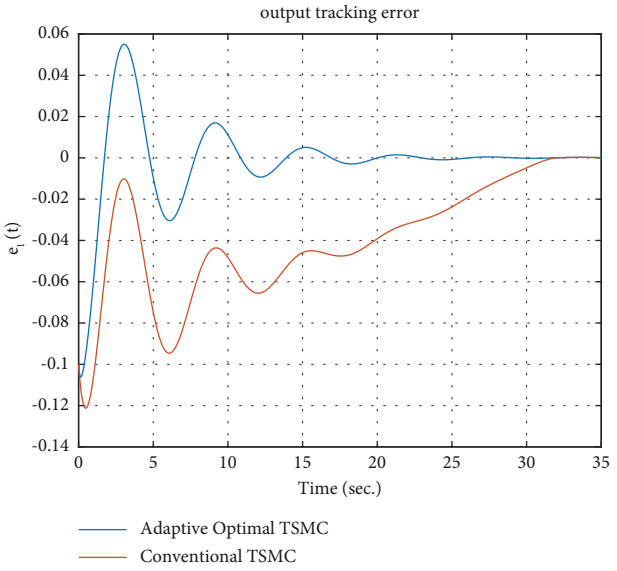

FIGURE 13: The trajectory of $e_1(t)$.

5. Conclusion and Future Works

This study presents an innovative strategy aimed at devising the optimal switching surface for implementing sliding mode control in a nonlinear system defined by TSFM. To achieve this objective, the approach involves the generation of a state feedback gain for each localized subsystem within the closed-loop setup. This gain is computed using a convex optimization strategy, which ensures the allocation of predetermined complex values with negative real components to a predefined number of eigenvalues, while simultaneously adhering to the H_2-norm criteria. Following the acquisition of the state feedback during the initial phase, the associated convex optimization problem is subsequently solved to ascertain the sliding surface. Notably, the suggested method offers several notable benefits. It takes into account the level of control efforts during the design of SMC and facilitates the adaptive determination of the nonlinear sliding surface gain based on trajectory conditions. The efficacy of this proposed approach is substantiated through simulation outcomes. In the realm of future research, potential avenues could encompass the development of effective techniques to address matched/unmatched uncertainty and the judicious selection of optimal TSMC parameters to ensure the attainment of the desired outcomes.

Data Availability

No data were used to support this study.

Conflicts of Interest

The authors declare that they have no conflicts of interest.

References

[1] M. Zheng, S. Yang, and L. Li, "Aperiodic sampled-data control for chaotic system based on takagi–sugeno fuzzy model," *Complexity*, vol. 2021, pp. 1–8, 2021.

[2] W. Wu, L. Zhang, Y. Wu, and H. Zhao, "Adaptive saturated two-bit-triggered bipartite consensus control for networked MASs with periodic disturbances: a low-computation method," *IMA Journal of Mathematical Control and Information*, vol. 17, 2024.

[3] A. Azizi, J. Tavoosi, and M. Shirkhani, "Control engineering solutions during epidemics: a review," *International Journal of Modelling, Identification and Control*, vol. 39, no. 2, pp. 97–106, 2021.

[4] Y. Yu, H.-K. Lam, and K. Y. Chan, "T–S fuzzy-model-based output feedback tracking control with control input saturation," *IEEE Transactions on Fuzzy Systems*, vol. 26, no. 6, pp. 3514–3523, 2018.

[5] J. Tavoosi, M. Shirkhani, A. Azizi, S. Ud Din, A. Mohammadzadeh, and S. Mobayen, "A hybrid approach for fault location in power distributed networks: impedance-

based and machine learning technique," *Electric Power Systems Research*, vol. 210, 2022.

[6] Y. Cao, B. Niu, H. Wang, and X. Zhao, "Event-based adaptive resilient control for networked nonlinear systems against unknown deception attacks and actuator saturation," *International Journal of Robust and Nonlinear Control*, vol. 34, no. 7, pp. 4769–4786, 2024.

[7] F. Soltanian and M. Shasadeghi, "Optimal sliding mode control design for constrained uncertain nonlinear systems using T–S fuzzy approach," *Iranian Journal of Science and Technology, Transactions of Electrical Engineering*, vol. 46, no. 2, pp. 549–563, 2022.

[8] B. Chen, J. Hu, Y. Zhao, and B. K. Ghosh, "Finite-time observer based tracking control of uncertain heterogeneous underwater vehicles using adaptive sliding mode approach," *Neurocomputing*, vol. 481, pp. 322–332, 2022.

[9] H. Li, J. Wang, H. Du, and H. R. Karimi, "Adaptive sliding mode control for Takagi–Sugeno fuzzy systems and its applications," *IEEE Transactions on Fuzzy Systems*, vol. 26, no. 2, pp. 531–542, 2018.

[10] Y. Zheng and G. Zhang, "Suboptimal control for nonlinear systems with disturbance via integral sliding mode control and policy iteration," *Journal of Optimization Theory and Applications*, vol. 185, no. 2, pp. 652–677, 2020.

[11] F. Soltanian, M. Shasadeghi, S. Mobayen, and A. Fekih, "Adaptive optimal multi-surface back-stepping sliding mode control design for the takagi-sugeno fuzzy model of uncertain nonlinear system with external disturbance," *IEEE Access*, vol. 10, pp. 14680–14690, 2022.

[12] S. Huang, G. Zong, N. Zhao, X. Zhao, and A. M. Ahmad, "Performance recovery-based fuzzy robust control of networked nonlinear systems against actuator fault: a deferred actuator-switching method," *Fuzzy Sets and Systems*, vol. 480, 2024.

[13] F. Soltanian, A. A. Alvanagh, and M. J. Khosrowjerdi, "Adaptive locally-linear-models-based fault detection and diagnosis for unmeasured states and unknown faults," in *Proceedings of the 2nd International Conference on Control, Instrumentation and Automation*, pp. 507–512, IEEE, Shiraz, Iran, December 2011.

[14] H. Li, J. Yu, C. Hilton, and H. Liu, "Adaptive sliding-mode control for nonlinear active suspension vehicle systems using T–S fuzzy approach," *IEEE Transactions on Industrial Electronics*, vol. 60, no. 8, pp. 3328–3338, 2013.

[15] H. Zhang, Q. Zou, Y. Ju, C. Song, and D. Chen, "Distance-based support vector machine to predict DNA N6-methyladenine modification," *Current Bioinformatics*, vol. 17, no. 5, pp. 473–482, 2022.

[16] F. Soltanian, A. A. Alvanagh, and M. J. Khosrowjerdi, "Adaptive locally-linear-models-based fault tolerant control for humanoid robot with unknown faults," in *Proceedings of the 20th Iranian Conference on Electrical Engineering (ICEE2012)*, pp. 1000–1005, IEEE, Tehran, Iran, May 2012.

[17] X. Yang, X. Wang, S. Wang, K. Wang, and M. B. Sial, "Finite-time adaptive dynamic surface synchronization control for dual-motor servo systems with backlash and time-varying uncertainties," *ISA Transactions*, vol. 137, pp. 248–262, 2023.

[18] M. Zhihong and X. H. Yu, "Terminal sliding mode control of MIMO linear systems," *IEEE Transactions on Circuits and Systems I: Fundamental Theory and Applications*, vol. 44, no. 11, pp. 1065–1070, 1997.

[19] C. Cao, J. Wang, D. Kwok et al., "webTWAS: a resource for disease candidate susceptibility genes identified by transcriptome-wide association study," *Nucleic Acids Research*, vol. 50, no. D1, pp. D1123–D1130, 2022.

[20] H. Komurcugil, "Adaptive terminal sliding-mode control strategy for DC–DC buck converters," *ISA Transactions*, vol. 51, no. 6, pp. 673–681, 2012.

[21] H. Mohammadi, A. Zare, M. Soltanolkotabi, and M. R. Jovanović, "Convergence and sample complexity of gradient methods for the model-free linear–quadratic regulator problem," *IEEE Transactions on Automatic Control*, vol. 67, no. 5, pp. 2435–2450, 2022.

[22] R. Aazami, M. Shoaei, A. Moradkhani, M. Shirkhani, A. Elrashidi, and K. M. AboRas, "Deep neural networks based method to islanding detection for multi-sources microgrid," *Energy Reports*, vol. 11, pp. 2971–2982, 2024.

[23] D. Fridovich-Keil, E. Ratner, L. Peters, A. D. Dragan, and C. J. Tomlin, "Efficient iterative linear-quadratic approximations for nonlinear multi-player general-sum differential games," in *Proceedings of the In 2020 IEEE international conference on robotics and automation (ICRA)*, pp. 1475–1481, Paris, France, May 2020.

[24] S. Danyali, A. Moradkhani, O. Abdulhussein Abdaumran, M. Shirkhani, and Z. Dadvand, "A novel multi-input medium-gain DC-DC boost converter with soft-switching performance," *International Journal of Electrical Power & Energy Systems*, vol. 155, 2024.

[25] P. Barsaiyan and S. Purwar, "Comparison of state feedback controller design methods for MIMO systems," in *Proceedings of the 2010 International Conference on Power, Control and Embedded Systems*, pp. 1–6, Allahabad, India, November 2010.

[26] M. Chilali and P. Gahinet, "H/sub ∞/design with pole placement constraints: an LMI approach," *IEEE Transactions on Automatic Control*, vol. 41, no. 3, pp. 358–367, 1996.

[27] A. Argha, S. W. Su, A. Savkin, and B. Celler, "Design of optimal sliding-mode control using partial eigenstructure assignment," *International Journal of Control*, vol. 92, no. 7, pp. 1511–1523, 2019.

[28] I. Halperin, G. Agranovich, and Y. Ribakov, "Extension of the constrained bilinear quadratic regulator to the excited multi-input case," *Journal of Optimization Theory and Applications*, vol. 184, no. 1, pp. 277–292, 2020.

[29] F. Thomas, A. V. Thottungal, and M. S. Johnson, "Composite control of a hovering helicopter based on optimized sliding mode control," *Journal of Optimization Theory and Applications*, vol. 191, no. 2-3, pp. 756–775, 2021.

[30] X. Yu, F. Liao, L. Li, and Y. Lu, "-," *Asian Journal of Control*, vol. 24, no. 2, pp. 626–641, 2021.

[31] X. Sun, Y. Gao, and C. Wu, "Output tracking control for a class of continuous-time T–S fuzzy systems," *Neurocomputing*, vol. 152, pp. 199–208, 2015.

[32] S. Pakkhesal and I. Mohammadzaman, "Less conservative output-feedback tracking control design for polynomial fuzzy systems," *IET Control Theory & Applications*, vol. 12, no. 13, pp. 1843–1852, 2018.

[33] X. Yang, X. Wang, S. Wang, and V. Puig, "Switching-based adaptive fault-tolerant control for uncertain nonlinear systems against actuator and sensor faults," *Journal of the Franklin Institute*, vol. 360, no. 16, pp. 11462–11488, 2023.

[34] L. Rajabpour, M. Shasadeghi, and A. Barzegar, *International Journal of Advanced Intelligence Paradigms*, vol. 14, no. 3/4, pp. 328–344, 2019.

[35] J. Yu, X. Dong, Q. Li, J. Lü, and Z. Ren, "Adaptive practical optimal time-varying formation tracking control for disturbed high-order multi-agent systems," *IEEE Transactions on*

Circuits and Systems I: Regular Papers, vol. 69, no. 6, pp. 2567–2578, 2022.

[36] G. Grimm, M. J. Messina, S. Tuna, and A. Teel, "Nominally robust model predictive control with state constraints," *42nd IEEE International Conference on Decision and Control (IEEE Cat. No. 03CH37475)*, vol. 2, pp. 1413–1418, 2003.

[37] J. Köhler, M. A. Müller, and F. Allgöwer, "A novel constraint tightening approach for nonlinear robust model predictive control," in *Proceedigs of the 2018 Annual American Control Conference (ACC)*, pp. 728–734, IEEE, Milwaukee, WI, USA, June 2018.

[38] J. Wang, C. Yang, J. Xia, Z.-G. Wu, and H. Shen, "Observer-based sliding mode control for networked fuzzy singularly perturbed systems under weighted try-once-discard protocol," *IEEE Transactions on Fuzzy Systems*, vol. 30, no. 6, pp. 1889–1899, 2022.

[39] J. Wang, J. Xia, H. Shen, M. Xing, and J. H. Park, "$\mathcal {H}_{\infty }$ synchronization for fuzzy Markov jump chaotic systems with piecewise-constant transition probabilities subject to PDT switching rule," *IEEE Transactions on Fuzzy Systems*, vol. 29, no. 10, pp. 3082–3092, 2021.

[40] J. Wang, J. Wu, H. Shen, J. Cao, and L. Rutkowski, "FuzzyH_∞Control of discrete-time nonlinear Markov jump systems via a novel hybrid ReinforcementQ-learning method," *IEEE Transactions on Cybernetics*, vol. 53, no. 11, pp. 7380–7391, 2023.

[41] F. Soltanian, M. Shasadeghi, S. Mobayen, and P. Skruch, "Output tracking control of a nonlinear system based on takagi-sugeno fuzzy model: generalized partial eigenstructure assignment approach," *IEEE Access*, vol. 12, pp. 18520–18535, 2024.

[42] G. Xingquan and G. Shuang, "LMI-based H2 control for TS fuzzy system with hard constraints," *International Journal of Control and Automation*, vol. 8, no. 3, pp. 21–30, 2015.

[43] C. Scherer and S. Weiland, "Linear matrix inequalities in control," *Lecture Notes, Dutch Institute for Systems and Control*, vol. 3, no. 2, 2000.

[44] A. Argha, S. W. Su, A. Savkin, and B. Celler, "2/H∞ based sliding mode control: a partial eigenstructure assignment method," in *Proceedings of the 2016 IEEE 55th conference on decision and control (CDC)*, pp. 5354–5359, Las Vegas, NV, USA, December 2016.

[45] P. Montagnon, "Stability of piecewise deterministic Markovian metapopulation processes on networks," *Stochastic Processes and Their Applications*, vol. 130, no. 3, pp. 1515–1544, 2020.

[46] V. Monjezi, A. Trivedi, G. Tan, and S. Tizpaz-Niari, "Information-theoretic testing and debugging of fairness defects in deep neural networks," in *Proceedings of the 2023 IEEE/ACM 45th International Conference on Software Engineering (ICSE)*, pp. 1571–1582, Melbourne, Australia, May 2023.

[47] S. Tizpaz-Niari, V. Monjezi, M. Wagner, S. Darian, K. Reed, and A. Trivedi, "Metamorphic testing and debugging of tax preparation software," in *Proceedings of the In 2023 IEEE/ACM 45th International Conference on Software Engineering: Software Engineering in Society (ICSE-SEIS)*, pp. 138–149, Melbourne, Australia, May 2023.

[48] L. Li and L. Yao, "Fault tolerant control of fuzzy stochastic distribution systems with packet dropout and time delay," *IEEE Transactions on Automation Science and Engineering*, pp. 1–10, 2024.

[49] C. Guo, J. Hu, J. Hao, S. Celikovsky, and X. Hu, "Fixed-time safe tracking control of uncertain high-order nonlinear pure-feedback systems via unified transformation functions," *Kybernetika*, pp. 342–364, 2023, https://arxiv.org/abs/2305.00505.

[50] Y. Shi, Q. Lan, X. Lan, J. Wu, T. Yang, and B. Wang, "Robust optimization design of a flying wing using adjoint and uncertainty-based aerodynamic optimization approach," *Structural and Multidisciplinary Optimization*, vol. 66, no. 5, p. 110, 2023.

[51] S. Ding, J. H. Park, and C. C. Chen, "Second-order sliding mode controller design with output constraint," *Automatica*, vol. 112, 2020.

[52] C. Zhang, L. Zhou, and Y. Li, "Pareto optimal reconfiguration planning and distributed parallel motion control of mobile modular robots," *IEEE Transactions on Industrial Electronics*, pp. 1–10, 2024.

[53] P. Tang, F. Zhang, J. Ye, and D. Lin, "An integral TSMC-based adaptive fault-tolerant control for quadrotor with external disturbances and parametric uncertainties," *Aerospace Science and Technology*, vol. 10, 2021.

[54] D. Tang, K. Xiao, G. Xiang et al., "On the nonlinear time-varying mixed lubrication for coupled spiral microgroove water-lubricated bearings with mass conservation cavitation," *Tribology International*, vol. 193, 2024.

[55] X. Liu, S. Lou, and W. Dai, "Further results on System identification of nonlinear state-space models," *Automatica*, vol. 148, 2023.